High Glucose Induces Mitochondrial Dysfunction in Retinal Müller Cells: Implications for Diabetic Retinopathy

Thomas Tien,[1] Joyce Zhang,[1] Tetsuya Muto,[1] Dongjoon Kim,[1] Vijay P. Sarthy,[2] and Sayon Roy[1]

[1]Departments of Medicine and Ophthalmology, Boston University School of Medicine, Boston, Massachusetts, United States
[2]Department of Ophthalmology, Northwestern University Feinberg School of Medicine, Chicago, Illinois, United States

Correspondence: Sayon Roy, Departments of Medicine and Ophthalmology, Boston University School of Medicine, 650 Albany Street, Boston, MA 02118, USA; sayon@bu.edu.

Submitted: January 5, 2017
Accepted: April 6, 2017

Citation: Tien T, Zhang J, Muto T, Kim D, Sarthy VP, Roy S. High glucose induces mitochondrial dysfunction in retinal Müller cells: implications for diabetic retinopathy. *Invest Ophthalmol Vis Sci*. 2017;58:2915–2921. DOI: 10.1167/iovs.16-21355

Purpose. To investigate whether high glucose (HG) induces mitochondrial dysfunction and promotes apoptosis in retinal Müller cells.

Methods. Rat retinal Müller cells (rMC-1) grown in normal (N) or HG (30 mM glucose) medium for 7 days were subjected to MitoTracker Red staining to identify the mitochondrial network. Digital images of mitochondria were captured in live cells under confocal microscopy and analyzed for mitochondrial morphology changes based on form factor (FF) and aspect ratio (AR) values. Mitochondrial metabolic function was assessed by measuring oxygen consumption rate (OCR) and extracellular acidification rate (ECAR) using a bioenergetic analyzer. Cells undergoing apoptosis were identified by differential dye staining and TUNEL assay, and cytochrome c levels were assessed by Western blot analysis.

Results. Cells grown in HG exhibited significantly increased mitochondrial fragmentation compared to those grown in N medium (FF = 1.7 ± 0.1 vs. 2.3 ± 0.1; AR = 2.1 ± 0.1 vs. 2.5 ± 0.2; $P < 0.01$). OCR and ECAR were significantly reduced in cells grown in HG medium compared to those grown in N medium (steady state: 75% ± 20% of control, $P < 0.02$; 64% ± 22% of control, $P < 0.02$, respectively). These cells also exhibited a significant increase (~2-fold) in the number of apoptotic cells compared to those grown in N medium ($P < 0.01$), with a concomitant increase in cytochrome c levels (247% ± 94% of control, $P < 0.05$).

Conclusions. Findings indicate that HG-induced mitochondrial morphology changes and subsequent mitochondrial dysfunction may contribute to retinal Müller cell loss associated with diabetic retinopathy.

Keywords: high glucose, diabetes, diabetic retinopathy, retinal Müller cells, mitochondria

The incidence and prevalence of diabetic retinopathy, the leading cause of blindness in the working-age population, is increasing worldwide.[1] Several studies have shown that retinal microvascular changes such as vascular cell loss and increased extravasation are triggered by HG conditions.[2–4] Furthermore, studies have established that hyperglycemic conditions affect retinal microvessel integrity and functionality, at least in part, by promoting apoptosis in endothelial cells, pericytes, and Müller cells that can compromise blood–retinal barrier (BRB) characteristics and ultimately lead to excess vascular permeability. We and others have shown that HG-induced mitochondrial dysfunction promotes apoptosis in retinal endothelial cells and pericytes, and contributes to retinal dysfunction.[5,6] However, it is unknown whether HG affects mitochondrial function and thereby promotes apoptosis in retinal Müller cells.

Müller cells, the principal glial cells in the retina, have an important role in maintaining the inner BRB[7,8] and supporting retinal neurons.[9] Retinal Müller cells have been shown to participate in the maintenance and regulation of BRB function.[10] Anatomically, retinal capillaries are in close contact with Müller cell processes,[11,12] which facilitate communication between the vasculature and neurons.[13] We have previously shown that under HG conditions, intercellular communication between rMC-1 and pericytes is compromised, at least in part, due to reduced Cx43 gap junctions, which may affect Müller cell and pericyte survival.[14] Metabolically, rMC-1 secrete factors such as pigment epithelium–derived growth factor, thromobospondin-1, and glial cell line–derived neurotrophic factor to enhance the barrier properties of the vascular endothelium.[15] However, in response to hypoxia or inflammation, Müller cells produce VEGF and tumor necrosis factor, which increase vascular permeability.[15] Therefore, the demise of retinal Müller cells could play a critical role in contributing to neuronal and vascular pathology in diabetic retinopathy.

An increasing number of studies have shown that diabetes induces Müller cell loss in rodent models of diabetic retinopathy. Previous studies have shown that after 7 months of diabetes, Müller cells are lost in the retinas of diabetic mice[16] and that Müller cell loss is associated with programmed cell death.[17–19] In vitro studies have shown that HG promotes Müller cell apoptosis by decreasing Akt activity.[20] Taken together, these studies provide evidence for Müller cell loss in the diabetic retina. However, mechanisms contributing to HG-induced Müller cell loss are unclear, and it is unknown whether mitochondrial dysfunction is involved in Müller cell loss.

Our previous studies have shown that HG-induced mitochondrial dysfunction promotes apoptosis in retinal endothelial cells and pericytes.[5,21] Oxidative stress from mitochondrial and nonmitochondrial sources have been reported to play a role in diabetes-associated osmotic swelling of Müller cells.[22] However, the specific role of changes in mitochondrial morphology and mitochondrial energy metabolism has not been investigated in

the context of Müller cell loss. As documented in our previous studies, HG induces mitochondrial fragmentation and thereby compromises mitochondrial functionality in retinal vascular cells.[5,6] Additionally, HG has been shown to induce mitochondrial morphology changes in various other cell types such as rat cardiomyoblasts[23] and human mesangial cells.[24] The purpose of the current study is to establish whether Müller cell loss is attributable to mitochondrial dysfunction by investigating the effects of HG on mitochondrial morphology; mitochondrial membrane potential heterogeneity; oxygen consumption rate (OCR); and extracellular acidification rate (ECAR) concomitant with cytochrome c release.

Methods

Cell Culture

We grew rMC-1 on poly-D-lysine coated, glass-bottom culture dishes (MatTek Corp., Ashland, MA, USA) in Dulbecco's modified Eagle's medium containing 10% fetal bovine serum (Sigma-Aldrich Corp., St. Louis, MO, USA); antimycotics; and antibiotics. To determine the effect of HG on mitochondrial morphology, rMC-1 were grown for 7 days under normal (5 mmol/L) or HG (30 mmol/L) conditions. In parallel, rMC-1 were grown in mannitol (30 mmol/L) for osmotic control. After 7 days of HG exposure, cells were subjected to mitochondrial staining and examined through live cell imaging using confocal microscopy.

Fluorescent Probes

To determine the effect of HG on mitochondrial morphology, rMC-1 grown in N or HG medium for 7 days were incubated at 37°C in a 5% CO_2 incubator with 30 nM membrane potential–dependent dye (MitoTracker Red [MTR] CMXRos; Invitrogen-Molecular Probes, Eugene, OR, USA) for 15 minutes before imaging and kept in medium during the imaging processes.

Confocal Microscopy

Live cell imaging of mitochondria was accomplished using a confocal microscope (Zeiss LSM 710-Live Duo; Carl Zeiss, Oberkochen, Germany) with a ×63 oil-immersion objective. Throughout the process, cells were incubated at 37°C in a 5% CO_2 humidified microscope stage chamber. We subjected MTR to 543-nm helium/neon laser excitation and emission was recorded through a band-pass 650- to 710-nm filter. Fields were randomly selected, and those with similar cell densities were then imaged. To observe individual mitochondria, *z*-stack images were taken in a series of 10 to 15 slices per cell with a thickness of 0.5 μm per slice.

Mitochondrial Morphology Analysis

Mitochondrial morphology was quantified using a computer-assisted morphometric analysis application to calculate form factor (FF) and aspect ratio (AR) values. Images of mitochondria were analyzed using Image J software (http://imagej.nih.gov/ij/; provided in the public domain by the National Institutes of Health, Bethesda, MD, USA) by first processing with a median filter to obtain isolated and equalized fluorescent pixels. Mitochondria were subjected to particle analysis to obtain FF values ($4\pi \times \text{area/perimeter}^2$) and AR values (ratio of the lengths of major and minor axes). Aspect ratio is a measure of mitochondrial length; a value of 1 indicates a perfect circle and increases with elongated and elliptical mitochondria. Form factor is an indication of both mitochondrial length and degree of mitochondrial branching. A form factor value of 1 reflects a circular, unbranched mitochondrion, while a higher FF value indicates a longer, more branched mitochondrion.

Cellular Oxygen Consumption and Extracellular Acidification

Oxygen consumption and extracellular acidification rates of rMC-1 were measured by a bioenergetic assay (XF 24; Seahorse Bioscience, Billerica, MA, USA). We plated and cultured rMC-1 in a 24-well microplate (Seahorse Bioscience) for 7 days in N or HG medium to assess cellular oxygen consumption and extracellular acidification rates. For analysis, growth medium was replaced with nonbuffered medium (XF Assay; Seahorse Bioscience) and cells were incubated at 37°C in a non-CO_2 incubator for 60 minutes to allow the temperature and pH to reach equilibrium. The bioenergetics assay (Seahorse Bioscience) was used to measure extracellular flux changes in oxygen and protons in the media immediately surrounding the cells. After steady-state oxygen consumption and extracellular acidification rates were obtained, ATP synthase inhibitor oligomycin (5 μM) and the proton ionophore FCCP (carbonyl cyanide-4-[trifluoromethoxy] phenylhydrazone; 1 μM), a mitochondrial uncoupler, were injected sequentially through reagent delivery chambers to each well in the microplate to obtain the maximum oxygen consumption rate. Finally, a mixture of 5 μM rotenone (a mitochondrial complex I inhibitor) and 5 μM antimycin A (an electron transport blocker) was injected to verify that observed changes were due mainly to mitochondrial respiration.

Mitochondrial Membrane Potential Heterogeneity Analysis

To examine mitochondrial membrane potential heterogeneity in rMC-1, a ratiometric image-analysis approach was applied based on dual staining, as previously described.[5] Tetramethylrhodamine ethyl ester (TMRE) is a quickly equilibrating membrane potential–dependent dye that does not inhibit mitochondrial respiration. MitoTracker Green (MTG; Thermo Fisher Scientific, Waltham, MA, USA) is a membrane potential–independent dye. Using the product ratio of TMRE to MTG dyes maintains the voltage dependency of TMRE. In addition, this ratio is independent of fluorescence intensity variability from one focal plane to another.[25]

Images were acquired using confocal microscopy and individual mitochondria were analyzed. Membrane potential heterogeneity was determined by the deviation in the ratio of TMRE (red; excitation/emission: 550 nm/574 nm) to MTG (green; excitation/emission: 490 nm/516 nm) fluorescence intensity for several mitochondria within each cell and was quantified using analytical software (Metamorph; Molecular Devices, Sunnyvale, CA, USA).

Cytochrome C Release

We washed rMC-1 grown in normal and HG with PBS and lysed with 0.1% Triton X-100 buffer containing 10 mmol/L Tris, pH 7.5, 1 mmol/L EDTA, and 1 mmol/L phenylmethylsulfonyl fluoride. The cellular extract was then centrifuged 700*g* for 5 minutes. The supernatant was extracted and centrifuged again at 21,000*g* for 15 minutes. The supernatant was extracted as the cytosolic protein fraction. The remaining cellular pellet was washed with the same Triton buffer and centrifuged at 21,000*g* for 15 minutes. The supernatant was discarded and the cellular pellet was washed with radioimmunoprecipitation assay buffer containing 1 mmol/L phenylmethylsulfonyl fluoride. The washed pellet solution was centrifuged at

Investigative Ophthalmology & Visual Science

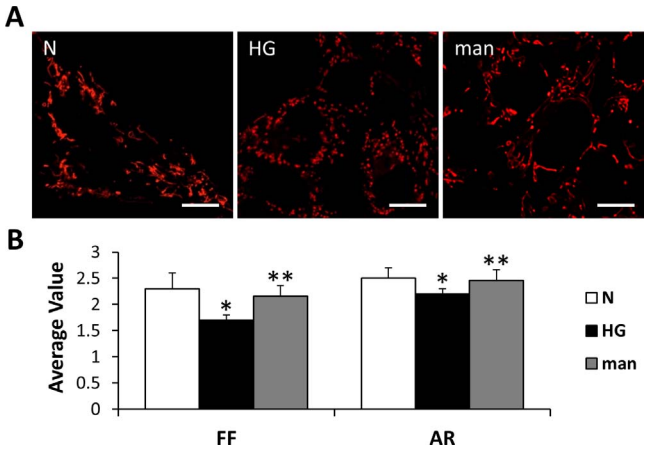

FIGURE 1. Mitochondrial morphology changes in rMC-1 grown in HG conditions. (**A**) Representative confocal images of rMC-1 grown in N or mannitol (man) medium and stained with MTR show long, tubular networks of mitochondria; rMC-1 grown in HG medium for 7 days show significant mitochondrial fragmentation. *Scale bars*: 10 μm. (**B**) Form factor and AR. The graph shows average FF and AR values for mitochondria of rMC-1 grown in N, HG, or man medium for 7 days. Mitochondrial fragmentation was significantly increased in rMC-1 grown in HG medium compared to that of cells grown in N medium as indicated by decreased FF and AR values. *N versus HG; $P < 0.01$, $n = 12$. **HG versus man; $P < 0.05$, $n = 12$.

21,000*g* for 15 minutes, and the supernatant was extracted as the mitochondrial protein fraction.

An equal volume of 2× sample buffer was added to the protein samples followed by denaturation at 95°C for 5 minutes. Then, the protein samples were electrophoresed at 120 V for 50 minutes. Kaleidoscope molecular weight standards were run in separate lanes in each gel. After completion of electrophoresis, the protein samples were transferred to nitrocellulose membranes using a semidry apparatus with Towbin buffer system according to the Towbin et al.[26] procedure. The membranes were blocked with 5% nonfat dry milk for 1 hour and then exposed to mouse anti-cytochrome c (cat. #Ms1192P0; NeoMarkers, Fremont, CA, USA); rabbit anti-VDAC1 (cat. #ab15895; Abcam, Cambridge, MA, USA); or rabbit anti-β-actin (cat. #4967; Cell Signaling, Danvers, MA, USA) in 0.2% nonfat milk overnight. After overnight incubation, the blots were washed with Tris-buffered saline containing 0.1% nonionic detergent (TWEEN 20; Sigma-Aldrich Corp.) and then incubated with anti-mouse or anti-rabbit IgG secondary antibody (Sigma-Aldrich Corp.) for 1 hour. The membrane was again washed as above, and then exposed to a chemiluminescent protein detection system (Immun-Star; Bio-Rad, Temecula, CA, USA) to detect the protein signals on an X-ray film. Densitometry was conducted and analyzed using ImageJ.

TUNEL Assay

To determine apoptosis, TUNEL assay was performed on rMC-1 grown in normal or HG medium for 7 days with a commercial kit (ApopTag In Situ Apoptosis Detection; Chemicon, Temecula, CA, USA) according to the manufacturer's instructions. Briefly, the cells were grown on coverslips, fixed with 4% paraformaldehyde, and permeated with a precooled mixture of a 2:1 ratio of ethanol/acetic acid. After two washes in PBS, slides were incubated with equilibration buffer and incubated with TdT enzyme in a moist chamber at 37°C for 1 hour. The cells were subsequently washed with PBS and incubated with anti-digoxigenin peroxidase. Finally, cells were then washed with PBS and mounted with reagent (SlowFade; Molecular Probes, Eugene, OR, USA). Images from 10 random fields representing each coverslip were captured using a digital microscope (DS-Fi1; Nikon Corp., Tokyo, Japan) and recorded for analysis.

Differential Dye Staining Assay

Apoptotic cells were determined using differential dye staining, based on the cell membrane's integrity to uptake fluorescent DNA binding dyes, ethidium bromide and acridine orange. We exposed rMC-1 grown on coverslips in N or HG medium for 7 days to a dye mixture containing 25 μg/mL ethidium bromide (Sigma-Aldrich Corp.) and 25 μg/mL acridine orange (Sigma-Aldrich Corp.) for 10 minutes, washed with PBS, fixed and mounted in a commercial reagent (SlowFade Antifade Kit; Invitrogen, Eugene, OR, USA). The cells were then visualized with a DAPI filter and at least 10 random fields were imaged using a digital camera attached to a fluorescence microscope (Diaphot; Nikon Corp.). The number of apoptotic cells per field was expressed as a percentage of the total number of cells in the field. Apoptotic cells appear orange or bright green while viable cells appear uniformly dark green.

Statistical Analysis

All data are expressed as the mean ± SD, and comparisons between the two groups were performed with Student's *t*-test. Comparisons between the three groups were performed using 1-way ANOVA followed by Tukey's post hoc test. A value of $P < 0.05$ was considered statistically significant.

Results

HG Exposure Induces Mitochondrial Network Fragmentation in rMC-1

We grew rMC-1 in N or HG medium for 7 days and stained with MTR before live examination by confocal microscopy to visualize the mitochondrial network. Mitochondrial network of rMC-1 grown in normal medium was interconnected and extensive throughout the cells. Individual mitochondria appeared long, tubular, and highly branched when grown in N conditions (Fig. 1A). However, the mitochondrial network of cells grown in HG conditions was significantly disturbed and scattered (Fig. 1A). Cells grown in HG medium had average FF and AR values that were significantly decreased compared with those grown in N medium (Fig. 1B; $P < 0.01$). Osmotic control using 30 mM mannitol for 7 days showed no change compared to those grown in normal condition (Figs. 1A, 1B).

HG Increases Membrane Potential Heterogeneity in Mitochondria of Müller Cells

To assess changes in mitochondrial membrane potential of Müller cells grown in HG medium for 7 days, rMC-1 were simultaneously stained with TMRE and MTG. Mitochondrial membrane potential heterogeneity was evaluated to investigate the distribution of mitochondrial membrane potential within individual cells. The fluorescence intensity deviation of several mitochondria within a single cell was measured, and Müller cells grown in HG showed greater variation in mitochondrial membrane potential, as seen by the greater range of TMRE and MTG overlap compared with those grown in normal medium (Fig. 2A). Mitochondrial membrane potential heterogeneity was significantly increased in Müller cells grown in HG for 7

Investigative Ophthalmology & Visual Science

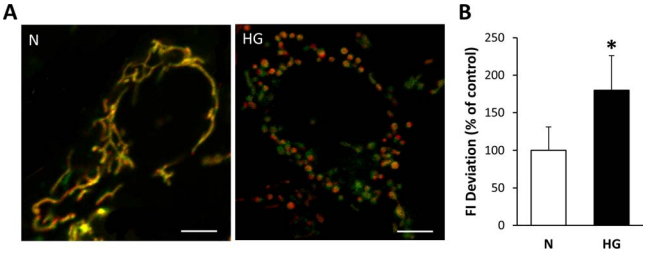

FIGURE 2. Mitochondrial membrane potential heterogeneity. Increase in mitochondrial membrane potential heterogeneity of rMC-1 grown in HG for 7 days. (**A**) Rat retinal Müller cells grown for 7 days in N or HG medium were double stained with mitochondrial membrane potential-sensitive TMRE (*red*) dye and membrane potential-independent MTG (*green*) dye. Mitochondria of rMC-1 grown in N medium are uniformly yellow, indicating little variation in membrane potential among the mitochondrial population, whereas mitochondria of rMC-1 grown in HG medium showed a greater variance in color (yellow, green, orange), indicating varied uptake of TMRE and heterogenic membrane potential within the mitochondrial network. *Scale bars*: 5 μm. (**B**) The graph shows the SD of the membrane potentials indicating significant increase in the heterogeneity of mitochondrial membrane potential. $^{*}P < 0.0005$, $n = 9$.

days compared with those grown in N medium (Fig. 2B; $P < 0.0005$).

HG Decreases Steady State, Maximal OCR and ECAR in rMC-1

To determine HG-induced changes to metabolic activity, rMC-1 grown in normal or HG conditions were measured for cellular oxygen consumption rates and extracellular acidification using the bioenergetic assay (Seahorse Bioscience). Rat retinal Müller cells grown in HG medium showed a significant decrease in steady state and maximal OCR compared to those grown in N medium (Fig. 3A; steady state OCR: 75% ± 20% of control, $P < 0.02$, $n = 5$; maximal OCR: 89.02% ± 23.76% of control, $P < 0.03$, $n = 5$). There was no significant difference in respiratory reserve. In addition, rMC-1 exposed to HG exhibited decreased ECAR compared to rMC-1 grown in N medium (Fig. 3B; 64% ± 22% of control, $P < 0.02$, $n = 4$) without significant difference in glycolytic capacity.

Cytochrome C Release and Increased Number of Apoptotic Cells Under HG Conditions

To determine whether changes in mitochondrial shape and metabolism were concomitant with increased apoptosis, mitochondrial protein fractions and cytosolic protein separated by differential centrifugation were analyzed by WB analysis for cytochrome c levels. Cells exposed to HG for 7 days showed a significant increase in cytochrome c levels in the cytosol (Figs. 4A, 4B; $P < 0.05$). Blots for β-actin in the mitochondrial fraction and VDAC-1 in the cytosolic fraction showed no visible bands.

Furthermore, to verify that cells exhibiting mitochondrial fragmentation and subsequent cytochrome c release are undergoing apoptosis under HG conditions, TUNEL assay and differential dye staining were performed in parallel. The number of TUNEL-positive cells was significantly increased in rMC-1 grown in HG compared with those grown in N medium (Figs. 5A, 5B; $P < 0.005$). Differential dye staining showed that the number of apoptotic cells was significantly increased in cells grown in HG medium (Figs. 5C, 5D; $P < 0.01$) compared to those grown in N medium.

DISCUSSION

In this study, we examined whether HG-induced mitochondrial morphology changes promote mitochondrial dysfunction and thereby contribute to Müller cell death. Our results indicate that HG exposure induces mitochondrial fragmentation and concomitantly increases membrane potential heterogeneity, decreases oxygen consumption rate, and decreases extracellular acidification rate. Importantly, these changes are concomitant with cytochrome c release and apoptosis of rMC-1, which suggests the possibility that mitochondrial dysfunction is involved in HG-induced Müller cell death.

Our results suggest that in the presence of HG, Müller cell mitochondria undergo fragmentation with altered mitochondrial membrane potential and lowered capacity for cellular respiration, as indicated by decreased steady state and maximal oxygen consumption. While cells grown in HG also showed significant decrease in basal ECAR, it is unclear if this difference was due to glycolysis alone or in conjunction with nonglycolytic processes. Interestingly, our results also suggest that rMC-1 grown in HG have preserved respiratory and glycolytic reserves concomitant with reductions in basal OCR and ECAR. Overall, these results suggest that the respiratory capacity of retinal Müller cells is compromised in HG conditions despite the cell maintaining a degree of metabolic reserve.

Although the exact mechanism underlying mitochondrial fragmentation in HG conditions is not completely understood, recent studies suggest that an alteration in mitochondrial fission-fusion dynamics may play an important role in compromising mitochondrial morphology. In vascular cells for instance, mitochondrial fragmentation was observed alongside an upregulation in mitochondrial fission proteins.[27] Other studies have suggested that changes in mitochondrial fission or fusion may alter mitochondrial respiration, membrane potential, and cytochrome c release.[28,29] More recently, studies have examined the possibility that compromised mitophagy, which is involved in the recycling of depolarized mitochondrial fragments,[30] may occur in diabetes and promote mitochondrial dysfunction.[31,32] Further studies are needed to identify specific fission and fusion genes that may be involved in HG- or diabetes-induced mitochondrial fragmentation, and to better understand mechanisms involving compromised mitophagy.

Our finding that mitochondrial dysfunction may underlie Müller cell loss under HG conditions complements an increasing body of studies that implicate the mitochondrion as a critical player in the pathogenesis of diabetic retinopathy.[5,21,33,34] Although it is well established that mitochondria are key components of energy homeostasis and critical regulators of apoptosis in various cell types, this is the first study that shows the involvement of HG-induced mitochondrial dysfunction in retinal Müller cells. Studies have shown that increased oxidative stress contributes to mitochondrial dysfunction and ultimately retinal vascular apoptosis,[33] and that mitochondrial superoxide dismutase may be protective against mitochondrial dysfunction.[35,36] A study emphasized the importance of mitochondrial structural and transport proteins in the retinas of diabetic rats and those of human eyes with diabetic retinopathy.[34] Additionally, studies have reported compromised mitochondrial function, such as cellular oxygen consumption under HG conditions.[5,21] Furthermore, evidence of mitochondrial DNA damage and epigenetic changes such as hypermethylation of mitochondrial DNA have also been reported in HG conditions and in patients with diabetic retinopathy.[37–39] Taken together, these findings suggest that mitochondrial abnormalities play a central role in the pathogenesis of diabetic retinopathy, and future therapies

Investigative Ophthalmology & Visual Science

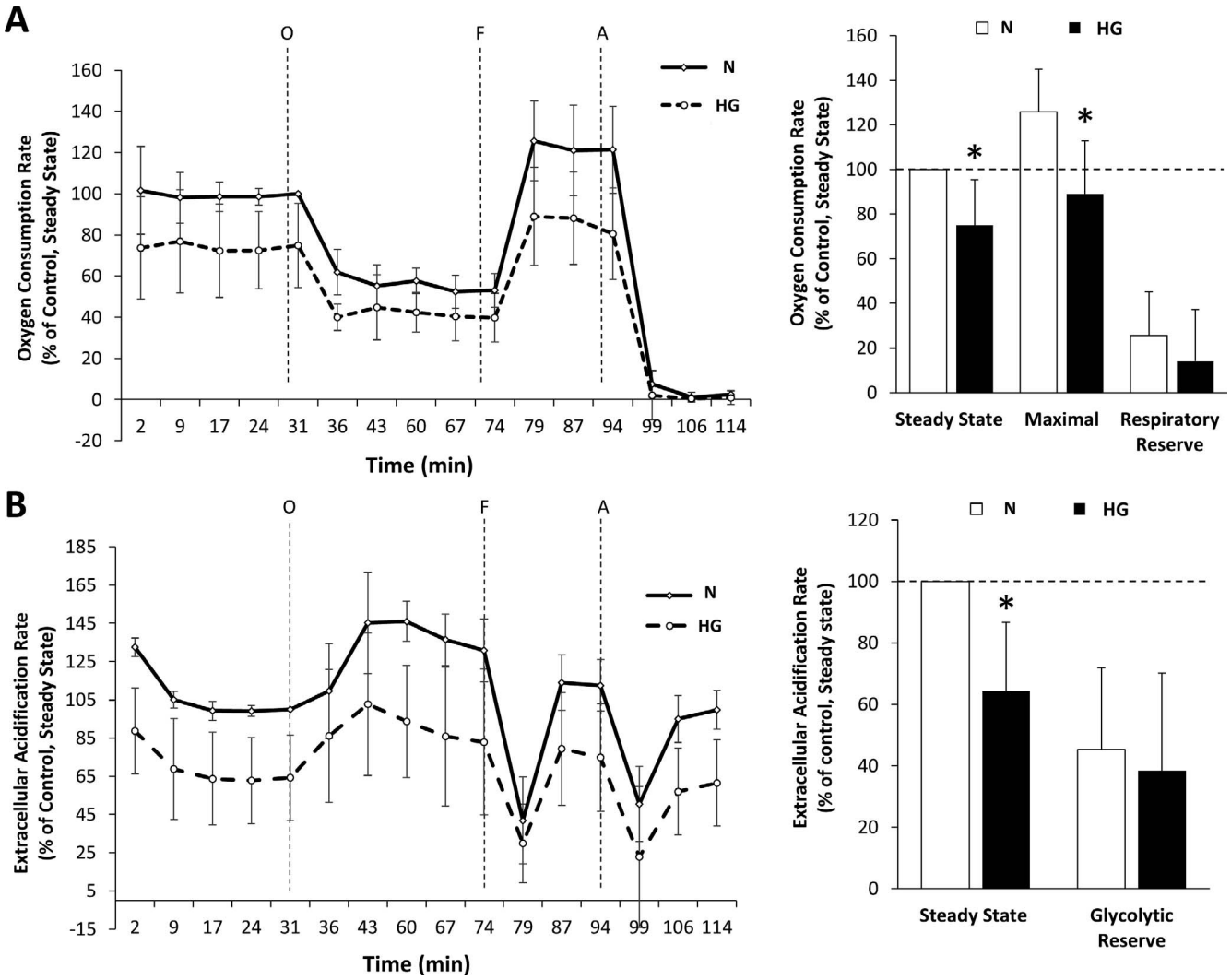

Figure 3. Effects of HG on OCR and ECAR in rMC-1. (**A**) Decreased OCR in rMC-1 grown in HG medium. Steady-state OCR and ECAR were measured at the fifth time point. Oligomycin (O) was injected to inhibit ATP synthase, with the addition of FCCP (F) to uncouple mitochondria and obtain maximal oxygen consumption rate at the 11th time point. Finally, rotenone and antimycin A were injected (A) to confirm that the respiration changes were due mainly to mitochondrial respiration. The line graph shows the cumulative OCR data for rMC-1 grown in normal or HG for 7 days. The oxygen consumption rate was significantly decreased under HG conditions compared to normal conditions in both steady state and maximal OCR. There was no significant difference in respiratory reserve. $^*P < 0.03$, $n = 5$. (**B**) Decreased ECAR in rMC-1 grown in HG medium. The line graph shows the cumulative ECAR data for rMC-1 grown in normal or HG for 7 days. Lines O, F, and A indicate injections of oligomycin, FCCP, and antimycin A/rotenone, respectively. Steady-state ECAR was significantly decreased under HG compared to N conditions. There was no significant difference in glycolytic reserve. $^*P < 0.02$, $n = 4$.

targeting mitochondrial processes may be of significant importance in treating this disease.

A limitation of the study is the use of a Müller cell line; as such, it is uncertain whether the phenomenon observed in the cell line occurs in in vivo conditions. However, an advantage in using rMC-1 is that several metabolic studies in the diabetic retinopathy field have established its authenticity and a recent study demonstrated that these cells exhibit retinal Müller cell characteristics.[40] In diabetes, it is certainly of interest to study mitochondrial morphologic changes in vivo. While it would be interesting to extend our findings with studies in an experimental animal model of diabetes, mitochondrial fragmentation can be determined in live cells in vitro using mito-specific dyes and live-cell confocal microscope imaging, and this approach is currently not suited to assess mitochondrial fragmentation in vivo.

In diabetic retinopathy, injury to or loss of retinal Müller cells may lead to disruption in the exchange of essential

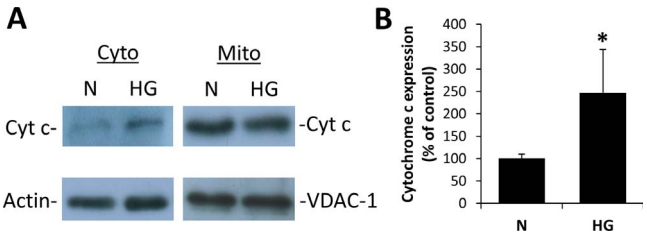

Figure 4. High glucose exposure increases cyt c levels in retinal Müller cells. (**A**) Cytosolic (cyto) and mitochondrial (mito) protein fractions were isolated from rMC-1 grown in N or HG medium for 7 days and cytochrome c release in the cytosol was assessed by Western blot analysis. Purity/loading of the mitochondrial fraction was confirmed by VDAC-1 staining, and purity/loading of the cytosolic fraction was confirmed by actin staining. (**B**) Graph illustration showing cumulative data of rMC-1 grown in HG medium for 7 days showed increased level of cytochrome c in the cytosol. Data are normalized to the actin signal. $^*P < 0.05$, $n = 4$.

Investigative Ophthalmology & Visual Science

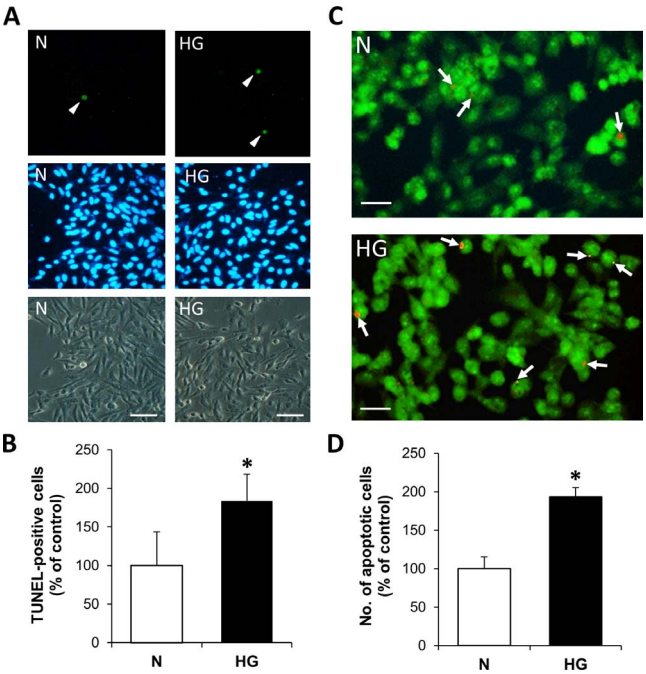

Figure 5. High glucose promotes apoptosis in retinal Müller cells. (**A**) TUNEL staining (*arrowhead*) of rMC-1 grown in N or HG medium for 7 days, with respective DAPI stain and phase-contrast image. *Scale bars*: 100 μm. (**B**) Under HG conditions, rMC-1 grown in HG showed a significant increase in the number of TUNEL-positive cells compared to those of normal cells. $^{*}P < 0.005$, $n = 4$. (**C**) Representative images of rMC-1 grown in N or HG medium subjected to differential dye staining. *Scale bars*: 50 μm. (**D**) Graph of cumulative data indicates rMC-1 grown in HG for 7 days shows significant increase in the number of apoptotic cells compared to those of N cells. $^{*}P < 0.01$, $n = 4$.

metabolic nutrients necessary to protect retinal neurons.[41] When Müller cells become activated and undergo reactive gliosis,[42] this protective mechanism may be compromised. Additionally, in response to diabetic pathologic changes, rMC-1 produce excess VEGF[43,44] promoting retinal inflammation, neovascularization, vascular leakage, and vascular lesions.[44] Such biochemical changes in rMC-1 and retinal neurons are irreversible; therefore, injury to Müller cells in the context of diabetic retinopathy will likely result in retinal damage and ultimately disrupt retinal homeostasis.[45] Findings from this study underscore the importance of mitochondrial function in Müller cell survival and that HG-induced changes in mitochondrial bioenergetics may promote Müller cell death in diabetic retinopathy.

Acknowledgments

Supported by National Institutes of Health EY018218 (SR), EY025528 (SR), the Undergraduate Research Opportunities Program award at Boston University (TT), the Medical Student Summer Research Program award at Boston University School of Medicine (TT), and an unrestricted grant from Research to Prevent Blindness, Inc.

Disclosure: **T. Tien**, None; **J. Zhang**, None; **T. Muto**, None; **D. Kim**, None; **V.P. Sarthy**, None; **S. Roy**, None

References

1. Lee R, Wong TY, Sabanayagam C. Epidemiology of diabetic retinopathy, diabetic macular edema and related vision loss. *Eye Vis (Lond)*. 2015;2:17.
2. Chronopoulos A, Tang A, Beglova E, Trackman PC, Roy S. High glucose increases lysyl oxidase expression and activity in retinal endothelial cells: mechanism for compromised extracellular matrix barrier function. *Diabetes*. 2010;59:3159–3166.
3. Chronopoulos A, Trudeau K, Roy S, Huang H, Vinores SA, Roy S. High glucose-induced altered basement membrane composition and structure increases trans-endothelial permeability: implications for diabetic retinopathy. *Curr Eye Res*. 2011;36:747–753.
4. Tien T, Barrette KF, Chronopoulos A, Roy S. Effects of high glucose-induced Cx43 downregulation on occludin and ZO-1 expression and tight junction barrier function in retinal endothelial cells. *Invest Ophthalmol Vis Sci*. 2013;54:6518–6525.
5. Trudeau K, Molina AJ, Roy S. High glucose induces mitochondrial morphology and metabolic changes in retinal pericytes. *Invest Ophthalmol Vis Sci*. 2011;52:8657–8664.
6. Bobbie MW, Roy S, Trudeau K, Munger SJ, Simon AM, Roy S. Reduced connexin 43 expression and its effect on the development of vascular lesions in retinas of diabetic mice. *Invest Ophthalmol Vis Sci*. 2010;51:3758–3763.
7. Tout S, Chan-Ling T, Hollander H, Stone J. The role of Müller cells in the formation of the blood-retinal barrier. *Neuroscience*. 1993;55:291–301.
8. Kaur C, Foulds WS, Ling EA. Blood-retinal barrier in hypoxic ischaemic conditions: basic concepts, clinical features and management. *Prog Retin Eye Res*. 2008;27:622–647.
9. Reichenbach A, Wurm A, Pannicke T, Iandiev I, Wiedemann P, Bringmann A. Müller cells as players in retinal degeneration and edema. *Graefes Arch Clin Exp Ophthalmol*. 2007;245:627–636.
10. Tretiach M, Madigan MC, Wen L, Gillies MC. Effect of Müller cell co-culture on in vitro permeability of bovine retinal vascular endothelium in normoxic and hypoxic conditions. *Neurosci Lett*. 2005;378:160–165.
11. Das A. Diabetic retinopathy: battling the global epidemic. *Indian J Ophthalmol*. 2016;64:2–3.
12. Holländer H, Makarov F, Dreher Z, van Driel D, Chan-Ling TL, Stone J. Structure of the macroglia of the retina: sharing and division of labour between astrocytes and Müller cells. *J Comp Neurol*. 1991;313:587–603.
13. Vecino E, Rodriguez FD, Ruzafa N, Pereiro X, Sharma SC. Glia-neuron interactions in the mammalian retina. *Prog Retin Eye Res*. 2016;51:1–40.
14. Muto T, Tien T, Kim D, Sarthy VP, Roy S. High glucose alters Cx43 expression and gap junction intercellular communication in retinal Müller cells: promotes Müller cell and pericyte apoptosis. *Invest Ophthalmol Vis Sci*. 2014;55:4327–4337.
15. Reichenbach A, Bringmann A. New functions of Müller cells. *Glia*. 2013;61:651–678.
16. Hammes HP, Federoff HJ, Brownlee M. Nerve growth factor prevents both neuroretinal programmed cell death and capillary pathology in experimental diabetes. *Mol Med*. 1995;1:527–534.
17. Hori S, Mukai N. Ultrastructural lesions of retinal pericapillary Müller cells in streptozotocin-induced diabetic rats. *Albrecht Von Graefes Arch Klin Exp Ophthalmol*. 1980;213:1–9.
18. Feenstra DJ, Yego EC, Mohr S. Modes of retinal cell death in diabetic retinopathy. *J Clin Exp Ophthalmol*. 2013;4:298.
19. Fu S, Dong S, Zhu M, et al. Müller glia are a major cellular source of survival signals for retinal neurons in diabetes. *Diabetes*. 2015;64:3554–3563.
20. Xi X, Gao L, Hatala DA, et al. Chronically elevated glucose-induced apoptosis is mediated by inactivation of Akt in cultured Müller cells. *Biochem Biophys Res Commun*. 2005;326:548–553.

21. Trudeau K, Molina AJ, Guo W, Roy S. High glucose disrupts mitochondrial morphology in retinal endothelial cells: implications for diabetic retinopathy. *Am J Pathol*. 2010;177:447–455.
22. Krugel K, Wurm A, Pannicke T, et al. Involvement of oxidative stress and mitochondrial dysfunction in the osmotic swelling of retinal glial cells from diabetic rats. *Exp Eye Res*. 2011;92:87–93.
23. Li K, Cui YC, Zhang H, et al. Glutamine reduces the apoptosis of H9C2 cells treated with high-glucose and reperfusion through an oxidation-related mechanism. *PLoS One*. 2015;10:e0132402.
24. Kang BP, Frencher S, Reddy V, Kessler A, Malhotra A, Meggs LG. High glucose promotes mesangial cell apoptosis by oxidant-dependent mechanism. *Am J Physiol Renal Physiol*. 2003;284:F455–F466.
25. Wikstrom JD, Katzman SM, Mohamed H, et al. beta-Cell mitochondria exhibit membrane potential heterogeneity that can be altered by stimulatory or toxic fuel levels. *Diabetes*. 2007;56:2569–2578.
26. Towbin H, Staehelin T, Gordon J. Electrophorectic transfer of proteins from polyacrylamide gels to nitrocellulose sheets: procedure and some applications. *Proc Natl Acad Sci U S A*. 1979;76:4350–4354.
27. Shenouda SM, Widlansky ME, Chen K, et al. Altered mitochondrial dynamics contributes to endothelial dysfunction in diabetes mellitus. *Circulation*. 2011;124:444–453.
28. Parone PA, Da Cruz S, Tondera D, et al. Preventing mitochondrial fission impairs mitochondrial function and leads to loss of mitochondrial DNA. *PLoS One*. 2008;3:e3257.
29. Frank S, Gaume B, Bergmann-Leitner ES, et al. The role of dynamin-related protein 1, a mediator of mitochondrial fission, in apoptosis. *Dev Cell*. 2001;1:515–525.
30. Twig G, Shirihai OS. The interplay between mitochondrial dynamics and mitophagy. *Antioxid Redox Signal*. 2011;14:1939–1951.
31. Soleimanpour SA, Ferrari AM, Raum JC, et al. Diabetes susceptibility genes Pdx1 and Clec16a function in a pathway regulating mitophagy in beta-cells. *Diabetes*. 2015;64:3475–3484.
32. Higgins GC, Coughlan MT. Mitochondrial dysfunction and mitophagy: the beginning and end to diabetic nephropathy? *Br J Pharmacol*. 2014;171:1917–1942.
33. Kowluru RA. Diabetic retinopathy: mitochondrial dysfunction and retinal capillary cell death. *Antioxid Redox Signal*. 2005;7:1581–1587.
34. Zhong Q, Kowluru RA. Diabetic retinopathy and damage to mitochondrial structure and transport machinery. *Invest Ophthalmol Vis Sci*. 2011;52:8739–8746.
35. Kowluru RA, Atasi L, Ho YS. Role of mitochondrial superoxide dismutase in the development of diabetic retinopathy. *Invest Ophthalmol Vis Sci*. 2006;47:1594–1599.
36. Kanwar M, Chan PS, Kern TS, Kowluru RA. Oxidative damage in the retinal mitochondria of diabetic mice: possible protection by superoxide dismutase. *Invest Ophthalmol Vis Sci*. 2007;48:3805–3811.
37. Cheng Z, Almeida FA. Mitochondrial alteration in type 2 diabetes and obesity: an epigenetic link. *Cell Cycle*. 2014;13:890–897.
38. Madsen-Bouterse SA, Mohammad G, Kanwar M, Kowluru RA. Role of mitochondrial DNA damage in the development of diabetic retinopathy, and the metabolic memory phenomenon associated with its progression. *Antioxid Redox Signal*. 2010;13:797–805.
39. Mishra M, Kowluru RA. Epigenetic Modification of Mitochondrial DNA in the development of diabetic retinopathy. *Invest Ophthalmol Vis Sci*. 2015;56:5133–5142.
40. Pfeffer BA, Xu L, Porter NA, Rao SR, Fliesler SJ. Differential cytotoxic effects of 7-dehydrocholesterol-derived oxysterols on cultured retina-derived cells: dependence on sterol structure, cell type, and density. *Exp Eye Res*. 2016;145:297–316.
41. Bringmann A, Pannicke T, Grosche J, et al. Müller cells in the healthy and diseased retina. *Prog Retin Eye Res*. 2006;25:397–424.
42. Dyer MA, Cepko CL. Control of Müller glial cell proliferation and activation following retinal injury. *Nat Neurosci*. 2000;3:873–880.
43. Pierce EA, Avery RL, Foley ED, Aiello LP, Smith LE. Vascular endothelial growth factor/vascular permeability factor expression in a mouse model of retinal neovascularization. *Proc Natl Acad Sci U S A*. 1995;92:905–909.
44. Wang JJ, Zhu M, Le YZ. Functions of Müller cell-derived vascular endothelial growth factor in diabetic retinopathy. *World J Diabetes*. 2015;6:726–733.
45. Garcia M, Vecino E. Role of Müller glia in neuroprotection and regeneration in the retina. *Histol Histopathol*. 2003;18:1205–1218.

Investigative Ophthalmology & Visual Science